Drug Delivery Hot Paper

International Edition: DOI: 10.1002/anie.201510844
German Edition: DOI: 10.1002/ange.201510844

Biodegradable Inorganic Nanovector: Passive versus Active Tumor Targeting in siRNA Transportation

*Dae-Hwan Park, Jaeyong Cho, Oh-Joon Kwon, Chae-Ok Yun, and Jin-Ho Choy**

Abstract: *The biodegradable inorganic nanovector based on a layered double hydroxide (LDH) holds great promise for gene and drug delivery systems. However, in vivo targeted delivery of genes through LDH still remains a key challenge in the development of RNA interference therapeutics. Here, we describe in vivo and in vitro delivery system for Survivin siRNA (siSurvivin) assembled with passive LDH with a particle size of 100 nm or active LDH conjugated with a cancer overexpressing receptor targeting ligand, folic acid (LDHFA), conferring them an ability to target the tumor by either EPR-based clathrin-mediated or folate receptor-mediated endocytosis. When not only transfected into KB cells but also injected into xenograft mice, LDHFA/siSurvivin induced potent gene silencing at mRNA and protein levels in vitro, and consequently achieved a 3.0-fold higher suppression of tumor volume than LDH/siSurvivin in vivo. This anti-tumor effect was attributed to a selectively 1.2-fold higher accumulation of siSurvivin in tumor tissue compared with other organs. Targeting to the tumor with inorganic nanovector can guide and accelerate an evolution of next-generation theranosis system.*

Harnessing the small interfering RNA (siRNA) therapeutics platform in genomic-based therapy for cancer treatment offers key benefits including evolutionary conserved sequence-specific target gene inhibition, at relatively lower concentration than those required for other conventional RNA based therapeutics.[1] In designing a fit-for-purpose siRNA delivery system with nanoparticles, it is required to improve biodistribution for the target site accumulation of nanoparticles and to facilitate degradation in their targets without causing off-target toxicities.[2–5] Most nanoparticles with a size of around 100 nm are expected to preferentially accumulate in the tumor tissue with a prolonged circulation time through passive tumor-targeting based on the enhanced permeability and retention (EPR) effect. Nevertheless, such passive targeting has typically resulted in phagocytic elimination by reticuloendothelial system (RES) uptake in both the liver and spleen. To improve systemic delivery, active tumor-targeting systems have been alternatively made, in which the surface of nanoparticles was functionalized with tumor-specific moieties that increase the affinity to tumor tissues and cancer cells, and subsequently could reduce off-target accumulations.

More than any other class of inorganic nanoparticles, layered double hydroxides (LDHs) with the general formula $[M^{2+}_{1-x}M^{3+}_{x}(OH)_2]^{x+}\cdot(A^n)_{x/n}\cdot mH_2O$ (where M = metal cations and A = interlayer anions) have gained considerable clinical attention mostly due to their biodegradability and potential to deliver functional biomolecules.[6] The first gene delivery system based on LDH was successfully introduced by Choy et al. in 2000,[6b] and this new LDH vector for gene therapy was also highlighted as a paradigm shift in thinking for non-viral vectors.[6c] Since then, a series of studies have shown that two-dimensional bio-inorganic nanohybrids can play a role in a drug delivery system with a controlled release manner.[7–9] Most reports have largely focused on in vitro release kinetics of drugs incorporated in LDHs,[7] but have also included investigations of cellular pathway mechanism, toxicities, and efficacy for chemo-therapy.[9] However, no design has been made so far to realize a tumor-targeted in vivo delivery system for siRNA through LDH. Herein, we describe the first attempt to demonstrate passive and active targeting strategies for siRNA-based gene therapy both in vitro and in vivo. We also fluorescently visualized each targeting functions and quantified the siRNA delivery activities of ligand-directed active targeting versus EPR-mediated passive targeting.

Passive targeting was performed by controlling the particle size of LDH nanovector with 100 nm. To enhance the therapeutic efficacy, active targeting was also designed by conjugating the folic acid (FA) onto the surface of LDH (LDHFA) to facilitate folate receptor (FR)-mediated uptake by cancer cells. We initiated our study by investigating the hybridization compatibility of LDH or LDHFA with siRNA. Survivin siRNA (siSurvivin) was chosen in our study for targeting proto-oncogene Survivin, a member of the inhibitor of apoptosis (IAP) gene family that induces cancer cell-specific cell death.[10] The layered structured LDH nanovector was prepared by co-precipitation and subsequent hydrothermal treatment. Activated FA was then coupled to the LDH through a silane coupling reaction (see Figure S1 A in the Supporting Information).[11] A fixed amount of siSurvivin stock solution was then added drop-wise to each colloidal suspension of LDH or LDHFA at different concentrations, and free siSurvivin was visualized by gel electrophoresis.

A self-assembly process driven by an electrostatic interaction between negatively charged siSurvivin and positively charged LDH and LDHFA at the weight ratio of 1:25 and

[*] Dr. D.-H. Park, M. Sc. J. Cho, Prof. Dr. J.-H. Choy
Center for Intelligent Nano-Bio Materials (CINBM), Department of Chemistry and Nano Science, Ewha Womans University
Seoul 120-750 (Republic of Korea)
E-mail: jhchoy@ewha.ac.kr
Dr. O.-J. Kwon, Prof. Dr. C.-O. Yun
Department of Bioengineering, College of Engineering, Hanyang University
Seoul 133-791 (Republic of Korea)

Supporting information for this article can be found under http://dx.doi.org/10.1002/anie.201510844.

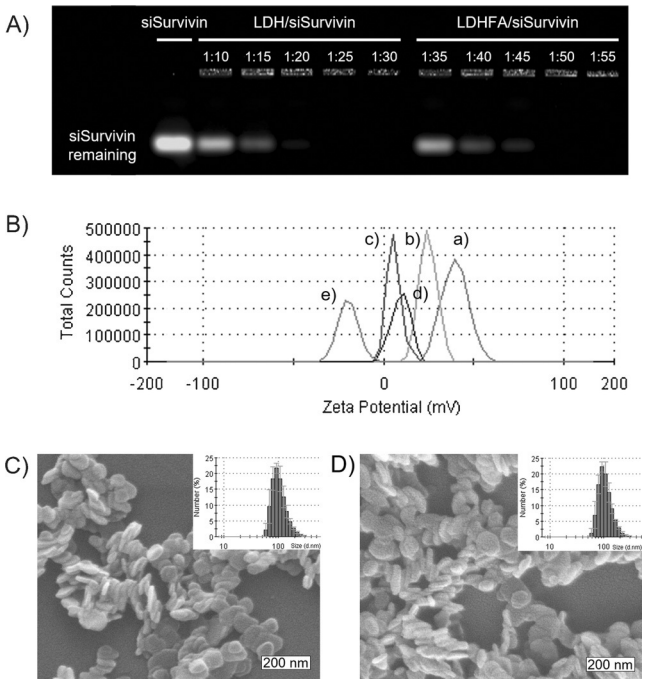

Figure 1. Chemical characterizations of LDH/siSurvivin and LDHFA/siSurvivin. A) Gel retardation assay for the assembly of siSurvivin with LDH or LDHFA at various weight ratio. B) Zeta potential analyses of a) LDH, b) LDHFA, c) LDH/siSurvivin, d) LDHFA/siSurvivin, and e) siSurvivin. SEM image and size distribution of C) LDH/siSurvivin and D) LDHFA/siSurvivin.

1:50, respectively (Figure 1A). At these ratios, LDH/siSurvivin and LDHFA/siSurvivin showed positive surface charges of $\xi = +9.6$ mV and $\xi = +7.9$ mV, respectively. This indicates that the negative charge of siSurvivin ($\xi = -19.5$ mV) was apparently neutralized by the positive surface charge of LDH ($+39.6$ mV) and LDHFA ($+24.7$ mV) (Figure 1B). Such a relatively low zeta potential of the nanohybrids would minimize an adsorption of proteins in blood vessels during prolonged circulation in vivo. UV/Vis spectra analysis also revealed that the characteristic absorbance peaks of LDH/siSurvivin and LDHFA/siSurvivin were slightly red-shifted after the hybridization due to the electrostatic interaction between siRNA and inorganic nanovectors as well as the scattering effect of LDH (Figure S1B). Each LDH/siSurvivin and LDHFA/siSurvivin exhibited fairly uniform hexagonal shaped platelets with a size of 100 nm as observed by scanning electron microscopy (SEM) and dynamic light scattering (DLS) analyses (Figure 1C,D).

The colloidal dispersion of both nanohybrids appeared to be stable in 10% mouse serum at physiological pH, although single particles with a diameter of slightly larger than 100 nm were observed due to the adsorption of serum proteins with a size of slightly smaller than 10 nm (Figure S1C). Furthermore, siSurvivin assembled with LDHFA was well protected from enzymatic degradation after treatment with RNase A at high concentration (Figure S1D). In the serum stability test for in vivo use of siSurvivin, the band brightness of siSurvivin assembled with LDHFA also demonstrated equivalent stability against blood nuclease digestion after incubation in 50% fetal bovine serum (FBS) with an estimated half-life of about 9 h. These relatively stable nanohybrids could thus be exploited for in vivo siRNA delivery to the tumor.

To evaluate in vitro efficacy of LDHFA/siSurvivin, FR-overexpressing KB cells and FR-negative A549 cells were transfected with each sample at FA-supplemented or FA-free condition, followed by quantitative real-time RT-PCR to analyze the Survivin gene expression. As shown in in vitro study, no cytotoxic effect was observed after treating with siRNA only, while the growth of cancer cell was clearly inhibited due to the higher transfection and enhanced therapeutic activity of the siRNA delivered by inorganic nanovector. The RT-PCR analysis indicated that both nanohybrids, respectively achieved more than 52% and approximately 28% decrease in Survivin mRNA expression compared to the control groups in KB and A549 cells. In KB cells, where the competition between free FA and LDHFA/siSurvivin over the receptor binding presumably occurred, 72% of Survivin mRNA expression was down-regulated by LDHFA/siSurvivin in FA free conditions while only 52% of Survivin expression was decreased when FA was presented during the treatment (Figure 2A). In A549 cells where FR is

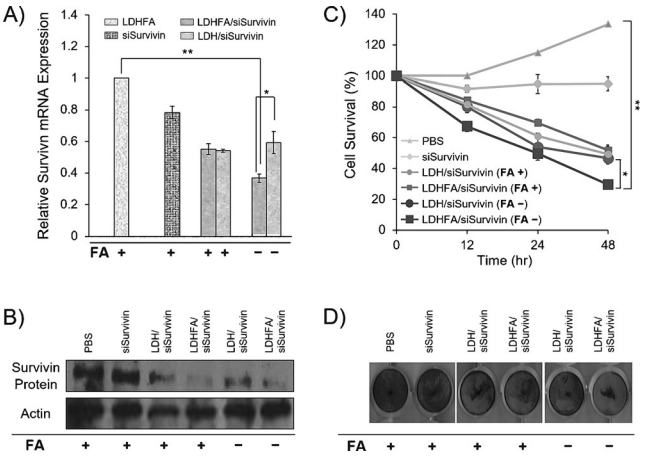

Figure 2. In vitro comparison of Survivin inhibition efficacy of LDH/siSurvivin and LDHFA/siSurvivin in KB cells in the presence or absence of free FA in the media. A) Quantitative real-time RT-PCR analysis of Survivin mRNA expression. B) Immunoblot analysis of Survivin protein expression. C) MTT reduction analysis on cell survival. D) Crystal violet staining image. *$p < 0.05$ versus LDH/siSurvivin-treated groups; **$p < 0.01$ versus PBS controls.

not expressed, both nanohybrids induced Survivin down-regulation to a similar extent (Figure S2A). In agreement with the results of RT-PCR analysis, nanohybrids treatment resulted in the reduction of Survivin protein expression, and the most significant change in the amounts of Survivin protein occurred in KB cells treated with LDHFA/siSurvivin in the absence of FA (Figure 2B and Figure S2B).

When facing competition for receptor binding or when there is no receptor to bind, the LDHFA nanovector, seems to passively select the unique cellular uptake route for the LDH nanovector, namely clathrin-mediated endocytosis, as demonstrated in our previous study.[8a,11] Furthermore, our results

are consistent with previous intracellular trafficking pathway study results indicating that the LDH nanovectors with a controlled particle size of 100 nm enhance the early-endosomal ($5.5 < pH < 6.5$) escape of therapeutic genes to be released into the cytosol.[12]

To demonstrate that post-translational regulation of Survivin by nanohybrids can have a significant effect on cancer cell proliferations, KB and A549 cells were transfected as indicated above and cell survival was measured by MTT assay. As shown in Figure 2C, only 20% of the KB cells treated with LDHFA/siSurvivin at FA-free conditions survived. In contrast, both FA-competing LDHFA/siSurvivin and LDH/siSurvivin, regardless of the presence of FA, gradually increased cell apoptosis resulting in an approximately 60% decrease in cell survival. In A549 cells, both nanohybrids decreased cell survival by 40% (Figure S2C). Crystal violet staining was also performed in parallel with MTT assay and the proliferation of KB cells was significantly inhibited by LDHFA/siSurvivin treatment in the absence of FA while the other group in both KB and A549 cells showed a moderate inhibition effect (Figure 2D and Figure S2D).

Given the sufficient decrease of Survivin expression at mRNA and protein levels and the increase in cellular apoptosis induced by nanohybrids, it is important to note that for a fixed incubation period, the in vitro efficacy of siSurvivin was significantly improved by LDHFA/siSurvivin than by LDH/siSurvivin in the FA-free environment. LDHFA/siSurvivin must compete with blood circulating FA to bind FR at the tumor surface in order to utilize the FR-mediated uptake pathway in vivo. Otherwise, it will passively accumulate at the tumor site due to the EPR effect similar to the LDH/siSurvivin. To address this issue, fluorescein-5-isothiocyanate (FITC)-conjugated nanohybrids were prepared.[11b,12a] The LDH-FITC/siSurvivin and LDHFA-FITC/siSurvivin were injected into KB tumor bearing nude mice via intraperitoneal (IP) route. At 30 minutes, 2 h, and 1 day after injection, the treated mice were sacrificed and the fluorescence intensity distributions of the nanohybrids in organs were analyzed using ex vivo optical imaging techniques (Figure S3). We visualized and quantified the accumulation of the nanohybrid particles in tumor tissue based on EPR-based versus receptor-mediated targeting function. At 30 minutes after injection, selected images are depicted in Figure 3A. Both LDH-FITC/siSurvivin and LDHFA-FITC/siSurvivin showed greater tumor selectivity over the other organs, including the lungs, liver and spleen which are known to be main sites for the accumulation of nanovectors. Fluorescence intensity in the tumors from LDHFA-FITC/siSurvivin treated mice was 1.2 fold higher than from LDH-FITC/siSurvivin treated mice, clearly confirming that LDHFA can competitively bind FR in vivo and can access more preferentially to the tumors than EPR-dependent LDH.

Moreover, different concentrations of the LDHFA/siSurvivin were also administered intraperioneally to balb/c mice, and the innate inflammatory responses and liver toxicity were assessed. As shown in Figure 3B, up to treatment with 2.5 mg kg^{-1} of LDHFA/siSurvivin, a dosage equals to 125 mg kg^{-1} of LDHFA, no significant elevation of inflammatory cytokine interleukin (IL)-6 (3.8 pg mL^{-}), alanine

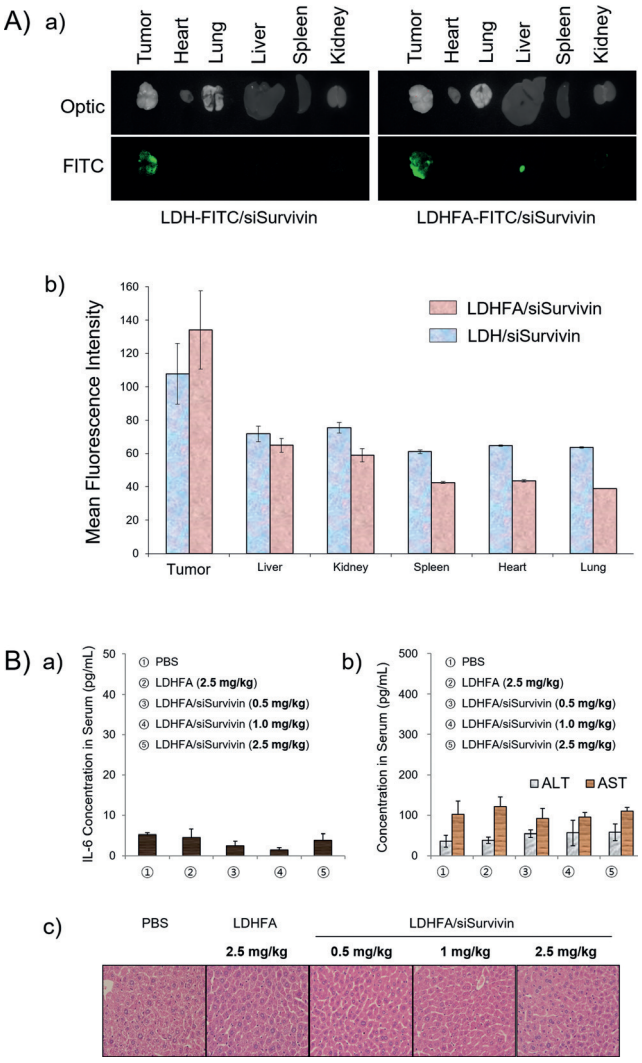

Figure 3. A) Ex vivo biodistribution of the LDH-FITC/siSurvivin and LDHFA-FITC/siSurvivin in the xenograft model. a) Optic and fluorescence images and b) quantitative analysis of tumor at 30 minutes after IP injection ($n = 3$ per group). B) Innate immune responses and liver toxicity of the LDHFA/siSurvivin treatment ($n = 4$ per group). a) Inflammatory cytokine level (IL-6 level) anaylzed at 6 h after LDHFA/siSurvivin treatement. b) ALT and AST levels. c) H&E staining of liver tissues perfomed at day 3 after treatment (original magnification: ×100).

transaminase (ALT) (57.7 pg mL^{-}) and aspartate transaminase (AST) (109.6 pg mL^{-}) were observed. Liver tissues were further analyzed by H&E staining and there were no signs of tissue damages. In vivo toxicity of LDHFA nanovector was evaluated to determine the therapeutic dosages and to measure the toxicity of LDHFA/siSurvivin. The results showed that the LDHFA nanovector was well tolerated in mice even at high concentrations (Figure S4). The LD_{50} (lethal dose 50%) value for LDHFA is more than 600 mg kg^{-1}, placing it in the non-toxic class. It indicated that the toxicity of inorganic LDHFA may correlate with the biodegradation to ionic species in vivo.

Once the therapeutic dosage of siRNA was determined to be a value of 2.5 mg kg^{-1} of siSurvivin per injection volume,

each sample of PBS (control), siSurvivin (2.5 mg), LDH/siSurvivin (62.5 mg/2.5 mg) and LDHFA/siSurvivin (125 mg/2.5 mg) was administered intraperioneally to the nude mice xenograft model bearing KB tumor, and then the tumor volumes were measured for 5 weeks to evaluate in vivo efficacy of the nanohybrids.

As shown in Figure 4A, on day 30 post-treatment, the mean sizes of tumor volumes in PBS and siSurvivin groups were 3176.61 mm^3 and 3194.72 mm^3, respectively. Interestingly, the LDHFA/siSurvivin treatment was shown to be more effective in supressing tumor growth, resulting in 66.4% decrease in tumor size compared to the control group (1067.05 mm^3; vs. PBS, $P < 0.01$). The LDH/siSurvivin treatment resulted in a 12% decrease in tumor size (2796.08 mm^3). It is worthy to note here that the inhibition rate of tumor growth in the LDHFA/siSurvivin with active targeting function achieved 3.0-fold higher level than that in the LDH/siSurvivin with passive targeting function. Furthermore, the survival curve for each treated group was generated based on the tumor growth. Mice treated with LDHFA/siSurvivin showed 83.3% survival on 32 days post-treatment. The LDH/siSurvivin treated mice also achieved 83.3% survival on 26 days post-treatment. However, the surviving mice were all dead on day 30 (Figure S5).

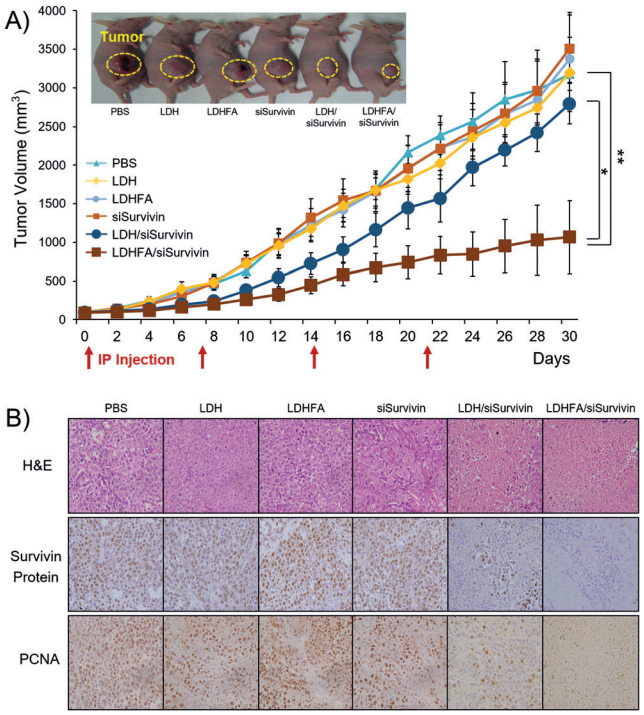

Figure 4. In vivo *anti*-tumor effect and Survivin down-regulation in tumors treated with each sample through IP route once every 7-days. A) Tumor growth inhibition ($n = 6$ per group). Tumor volumes were measured at 2-days interval. Tumor sizes are presented as means ± SE. *$p < 0.05$ versus LDH/siSurvivin treated group; ** $p < 0.01$ versus PBS-treated group (Inset photo image shows the mice on 18 days post-treatment. Tumor growth rate with LDHFA/siSurvivin was significantly slower, resulting in a tumor volume of 583 mm^3, which was remarkably smaller than the values in other groups: 1693 mm^3 (PBS); 1474 mm^3 (siSurvivin); 1157 mm^3 (LDH/siSurvivin)). B) H&E, Survivin protein and PCNA stained tumor tissue section ($n = 3$ per group) (original magnification: ×100).

Survivin antibody staining showed a low level of Survivin protein expression in tumors from nanohybrids groups (Figure 4B). The same specimen also had a low level of proliferating cell nuclear antigen (PCNA) and appeared to be undergoing tumor cell necrosis, as assessed by H&E staining. These results support the in vitro data showing that LDHFA/siSurvivin efficiently suppresses Survivin expression both at the post-transcriptional and -translational levels, inducing necrosis in cancer cells. The LDH/siSurvivin also decreased Survivin protein expression to a lesser extent, resulting in apoptosis in tumors.

In summary, we successfully demonstrated, for the first time, in vivo tumor-specific siRNA delivery system and cancer therapeutic efficacy employing the ligand-directed active targeting function of 100 nm sized LDHFA nanovector in comparison with their passive targeting counterpart, LDH nanovector. The in vitro and in vivo study results showed that the LDHFA/siSurvivin was able to bypass multiple biological barriers, including blocking blood nuclease digestion, improving tumor-targeted biodistribution through the EPR effect, and enhancing endocytosis by increasing cell binding through ligand and cancer-cell receptors, prompting early endosomal escape of siSurvivin to the cytosol for target mRNA silencing. In the future work on LDH nanosystem, dual targeting delivery to tumor cells and other interesting targets should be developed for intelligent gene therapy through advanced cogno-manipulation that can communicate with molecular interaction.

Acknowledgements

This work was supported by a National Research Foundation of Korea (grant number NRF) Grant funded by the Korean Government (MSIP; grant number 2005-0049412).

Keywords: cancer therapy · inorganic nanovectors · nanoparticles · layered compounds · siRNA delivery

How to cite: *Angew. Chem. Int. Ed.* **2016**, *55*, 4582–4586
Angew. Chem. **2016**, *128*, 4658–4662

[1] a) J. Kurreck, *Angew. Chem. Int. Ed.* **2009**, *48*, 1378–1398; *Angew. Chem.* **2009**, *121*, 1404–1426; b) H. Yin, R. L. Kanasty, A. A. Eltoukhy, A. J. Vegas, J. R. Dorkin, D. G. Anderson, *Nat. Rev. Genet.* **2014**, *15*, 541–555.

[2] a) K. Brunner et al., *Angew. Chem. Int. Ed.* **2015**, *54*, 1946–1949; *Angew. Chem.* **2015**, *127*, 1968–1971; b) F. Perche, S. Biswas, T. Wang, L. Zhu, V. P. Torchilin, *Angew. Chem. Int. Ed.* **2014**, *53*, 3362–3366; *Angew. Chem.* **2014**, *126*, 3430–3434.

[3] a) J. H. Lee, K. Lee, S. H. Moon, Y. Lee, T. G. Park, J. Cheon, *Angew. Chem. Int. Ed.* **2009**, *48*, 4174–4179; *Angew. Chem.* **2009**, *121*, 4238–4243; b) J. Shi, Z. Xiao, A. R. Votruba, C. Vilos, O. C. Farokhzad, *Angew. Chem. Int. Ed.* **2011**, *50*, 7027–7031; *Angew. Chem.* **2011**, *123*, 7165–7169.

[4] a) H. Koo, M. S. Huh, I. C. Sun, S. H. Yuk, K. Choi, K. Kim, I. C. Kwon, *Theor. Chem. Acc. Acc. Chem. Res.* **2011**, *44*, 1018–1028; b) K. A. Whitehead et al., *Nat. Commun.* **2014**, *5*, 4277.

[5] a) C. J. Cheng, G. T. Tietjen, J. K. Saucier-Sawyer, W. M. Saltzman, *Nat. Rev. Drug Discovery* **2015**, *14*, 239 – 247; b) S. Kunjachan et al., *Nano Lett.* **2014**, *14*, 972 – 981.

[6] a) J. H. Choy, S. Y. Kwak, J. S. Park, Y. J. Jeong, J. Portier, *J. Am. Chem. Soc.* **1999**, *121*, 1399 – 1400; b) J. H. Choy, S. Y. Kwak, Y. J. Jeong, J. S. Park, *Angew. Chem. Int. Ed.* **2000**, *39*, 4041 – 4045; *Angew. Chem.* **2000**, *112*, 4207 – 4211; c) D. Adam, *Nature* **2000**, DOI: 10.1038/news001123-1; d) V. Sokolova, M. Epple, *Angew. Chem. Int. Ed.* **2008**, *47*, 1382 – 1395; *Angew. Chem.* **2008**, *120*, 1402 – 1416; e) K. Ariga, Q. Ji, M. J. McShane, Y. M. Lvov, A. Vinu, J. P. Hill, *Chem. Mater.* **2012**, *24*, 728 – 737.

[7] a) D. H. Park, S. J. Hwang, J. M. Oh, J. H. Yang, J. H. Choy, *Prog. Polym. Sci.* **2013**, *38*, 1442 – 1486; b) J. M. Oh, T. T. Biswick, J. H. Choy, *J. Mater. Chem.* **2009**, *19*, 2553 – 2563; c) A. I. Khan, L. Lei, A. J. Norquist, D. O'Hare, *Chem. Commun.* **2001**, 2342 – 2343.

[8] a) J. M. Oh, S. J. Choi, S. T. Kim, J. H. Choy, *Bioconjugate Chem.* **2006**, *17*, 1411 – 1417; b) S. J. Choi, J. H. Choy, *J. Mater. Chem.* **2011**, *21*, 5547 – 5554; c) G. Choi, O. J. Kwon, Y. Oh, C. O. Yun, J. H. Choy, *Sci. Rep.* **2014**, *4*, 4430; d) L. Wang et al., *Biomaterials* **2013**, *34*, 3390 – 3401.

[9] a) L. Desigaux et al., *Nano Lett.* **2006**, *6*, 199 – 204; b) D. H. Park, J. E. Kim, J. M. Oh, Y. G. Shul, J. H. Choy, *J. Am. Chem. Soc.* **2010**, *132*, 16735 – 16736; c) S. Li et al., *J. Mater. Chem. B* **2013**, *1*, 61 – 68; d) L. Li, W. Gu, J. Chen, W. Chen, Z. P. Xu, *Biomaterials* **2014**, *35*, 3331 – 3339.

[10] a) G. Ambrosini et al., *Nature* **1997**, *3*, 917 – 921; b) D. C. Altieri, *Nat. Rev. Cancer* **2003**, *3*, 46 – 54; c) B. R. Han, H. O. Park, M. S. Shin, S. Y. Lee, US8779114 B2, Jul. 15, **2014**; d) T. Y. Lee et al., *Mol. Cells* **2013**, *35*, 320 – 326.

[11] a) J. M. Oh, S. J. Choi, G. E. Lee, S. H. Han, J. H. Choy, *Adv. Funct. Mater.* **2009**, *19*, 1617 – 1624; b) J. M. Oh, S. J. Choi, G. E. Lee, J. E. Kim, J. H. Choy, *Chem. Asian J.* **2009**, *4*, 67 – 73.

[12] a) H. E. Chung, D. H. Park, J. H. Choy, S. J. Choi, *Appl. Clay Sci.* **2012**, *65*, 24 – 30; b) J. Gilleron et al., *Nat. Biotechnol.* **2013**, *31*, 638 – 646; c) D. Ma, *Nanoscale* **2014**, *6*, 6415 – 6425.

Received: November 23, 2015
Published online: February 16, 2016

